HHS Public Access

Author manuscript

Mamm Genome. Author manuscript; available in PMC 2022 December 19.

Published in final edited form as:

Mamm Genome. 2022 December ; 33(4): 575–589. doi:10.1007/s00335-022-09957-w.

An interaction of inorganic arsenic exposure with body weight and composition on type 2 diabetes indicators in Diversity Outbred mice

James G. Xenakis[1,6], **Christelle Douillet**[2], **Timothy A. Bell**[1], **Pablo Hock**[1], **Joseph Farrington**[1], **Tianyi Liu**[3], **Caroline E. Y. Murphy**[1], **Avani Saraswatula**[1], **Ginger D. Shaw**[1,4], **Gustavo Nativio**[5], **Qing Shi**[2], **Abhishek Venkatratnam**[2,5], **Fei Zou**[3], **Rebecca C. Fry**[5,6,7], **Miroslav Stýblo**[2,6,7], **Fernando Pardo-Manuel de Villena**[1,4]

[1]Department of Genetics, School of Medicine, The University of North Carolina at Chapel Hill, Chapel Hill, NC 27599, USA

[2]Department of Nutrition, Gillings School of Global Public Health, The University of North Carolina at Chapel Hill, Chapel Hill, NC 27599, USA

[3]Department of Biostatistics, Gillings School of Global Public Health, The University of North Carolina at Chapel Hill, Chapel Hill, NC 27599, USA

[4]Lineberger Comprehensive Cancer Center, The University of North Carolina at Chapel Hill, Chapel Hill, NC 27599, USA

[5]Department of Environmental Science and Engineering, Gillings School of Global Public Health, The University of North Carolina at Chapel Hill, Chapel Hill, NC 27599, USA

[6]Curriculum in Toxicology and Environmental Medicine, The University of North Carolina at Chapel Hill, Chapel Hill, NC 27599, USA

[7]Institute for Environmental Health Solutions, The University of North Carolina at Chapel Hill, Chapel Hill, NC 27599, USA

Abstract

Type 2 diabetes (T2D) is a complex metabolic disorder with no cure and high morbidity. Exposure to inorganic arsenic (iAs), a ubiquitous environmental contaminant, is associated with increased T2D risk. Despite growing evidence linking iAs exposure to T2D, the factors underlying inter-individual differences in susceptibility remain unclear. This study examined the interaction between chronic iAs exposure and body composition in a cohort of 75 Diversity Outbred mice. The study design mimics that of an exposed human population where the genetic diversity of the mice provides the variation in response, in contrast to a design that includes untreated mice. Male mice were exposed to iAs in drinking water (100 ppb) for 26 weeks. Metabolic indicators used as

✉Rebecca C. Fry, rfry@unc.edu, Miroslav Stýblo, miroslav_styblo@med.unc.edu, Fernando Pardo-Manuel de Villena, fernando_pardo-manuel@med.unc.edu.

Conflict of interest The authors have no competing interests to declare that are relevant to the content of this article.

Supplementary Information The online version contains supplementary material available at https://doi.org/10.1007/s00335-022-09957-w.

diabetes surrogates included fasting blood glucose and plasma insulin (FBG, FPI), blood glucose and plasma insulin 15 min after glucose challenge (BG15, PI15), homeostatic model assessment for β-cell function and insulin resistance (HOMA-B, HOMA-IR), and insulinogenic index. Body composition was determined using magnetic resonance imaging, and the concentrations of iAs and its methylated metabolites were measured in liver and urine. Associations between cumulative iAs consumption and FPI, PI15, HOMA-B, and HOMA-IR manifested as significant interactions between iAs and body weight/composition. Arsenic speciation analyses in liver and urine suggest little variation in the mice's ability to metabolize iAs. The observed interactions accord with current research aiming to disentangle the effects of multiple complex factors on T2D risk, highlighting the need for further research on iAs metabolism and its consequences in genetically diverse mouse strains.

Introduction

Type 2 diabetes (T2D) is a complex metabolic disorder currently affecting hundreds of millions of individuals worldwide (Stanton et al. 2015; U.S. Department of Health And Human Services 2007). There is no cure for T2D and it is associated with high morbidity and mortality, resulting in more than one million deaths annually (Roglic and World Health Organization 2016). The prevalence of T2D has almost doubled since 1980 (Roglic and World Health Organization 2016), with around 9% of the U.S. population currently affected—a proportion that is estimated to rise to 30% by 2050 (CDC 2020). In the U.S., the estimated health expenditure for T2D and related diseases in 2015 was over $320 billion (Babu et al. 2007; Maull et al. 2012). Despite recent advances in research on T2D etiology, the biological mechanisms underlying the basic metabolic defects remain poorly understood. While an increase in obesity is the main driver of the rise of T2D prevalence, particularly in children (Fujimoto and Polonsky 2009; Mayer-Davis et al. 2017), obesity alone does not explain the current T2D epidemic. Growing evidence suggests that exposures to environmental pollutants, including naturally occurring and anthropogenic chemicals, which can act as obesogens and/or diabetogens, are contributing factors (Heindel et al. 2017).

One such chemical is inorganic arsenic (iAs), a ubiquitous contaminant of both drinking water and food that is currently poisoning hundreds of millions of people worldwide (Cubadda et al. 2017; IARC 2004). The health consequences of chronic exposure to iAs are complex. In addition to being a human carcinogen, iAs is associated with a variety of dermal, cardiometabolic, and respiratory disorders (U.S. Department of Health And Human Services 2007). Toxicologists have implicated iAs exposure in the risk of T2D, an association that has been born out in multiple study designs and at a range of doses. (Agusa et al. 2011; Kuo et al. 2013; St-Onge et al. 2004; Sumi and Himeno 2012). While the association between iAs exposure and T2D is well established and some of the potential mechanisms identified, little is known about factors that determine inter-individual variation in susceptibility to iAs-associated T2D. One important factor is the process by which iAs is metabolized into the methylated metabolites monomethyl-arsenic (MMAs) and dimethylarsenic (DMAs). This process is catalyzed by arsenic (+ 3 oxidation state) methyltransferase (AS3MT) (Maull et al. 2012). While the AS3MT-catalyzed methylation of

iAs is essential for body clearance of iAs, the methylated metabolites that contain trivalent arsenic ($MMAs^{III}$ and $DMAs^{III}$) inhibit processes that regulate glucose metabolism in a manner consistent with diabetes (Castriota et al. 2020; Martin et al. 2017; Maull et al. 2012). In humans, polymorphisms in the *AS3MT* gene have been associated with variability in iAs metabolism, and several studies have suggested that polymorphisms in *AS3MT* and other genes involved in iAs metabolism or in the regulation of glucose homeostasis may be risk factors for iAs-associated T2D (Douillet et al. 2021; Drobná et al. 2013; Lindberg et al. 2007; Martin et al. 2017; Su et al. 2012). A better understanding of the degree to which these polymorphisms are associated with differences in susceptibility to T2D in populations exposed to iAs is of pressing import, given the likely implication of iAs in the increasing prevalence and burden of T2D.

While the independent effects of obesity and iAs metabolism on T2D risk are themselves of interest, understanding the interplay between these factors is also of great interest to environmental toxicologists. Obesity has been shown to modify iAs metabolism in population and laboratory studies (Lin et al. 2014; Lindberg et al. 2007; Su et al. 2012). Because iAs metabolism plays a key role in the susceptibility to adverse effects of iAs exposure, it is likely that obesity can modify the diabetogenic effects of iAs exposure by modifying iAs metabolism. In addition, obesity may act additively with iAs exposure to impair glucose homeostasis. Indeed, a recent study in Chile has shown that obese individuals are at higher risk of developing T2D compared to lean individuals when exposed to iAs (Castriota et al. 2018). However, detailed information about the interaction between iAs exposure and obesity in the context of diabetes and about the role of genetics in this interaction is lacking.

In the present study, we examined the diabetogenic effects of chronic iAs exposure in a cohort of 75 male Diversity Outbred (DO) mice that were exposed to 100 ppb iAs in drinking water for 26 weeks. The DO are a valuable resource for this study, as their phenotypic and genetic diversity make them a powerful model of human disease (Chesler et al. 2016; Churchill et al. 2012). The DO have been shown to manifest wide phenotypic variability over a range of basal phenotypes (Logan et al. 2013; Svenson et al. 2012) including many specifically relevant to toxicology (Harrill et al. 2018). They have further been shown to display a wide range of phenotypic variability in response to various experimental treatments (French et al. 2015; Kurtz et al. 2020; Mayeux et al. 2018; Patterson et al. 2020; Recla et al. 2019). Thus, they were anticipated to manifest an expanded range of phenotypic variability compared to standard inbred lines typically used in arsenic research. Likewise, they were anticipated to exhibit wide variability in their capacity to metabolize iAs (Keele et al. 2020). While these features made the DO an attractive resource for our study, they also cause it to come with an attendant limitation: the genetic uniqueness of each sample precludes the inclusion of genetic controls. As a result, unlike the randomized trial setting wherein potential confounders are guaranteed to be balanced across treatment groups (in expectation), care must be taken to control for them, as in a population or a retrospective database analysis. Throughout the course of the study, we examined a range of metabolic indicators that serve as surrogates for T2D, while also measuring body composition and the concentrations of iAs and its methylated metabolites (MMAs and DMAs) in liver and urine.

Materials and methods

Mice and treatment

A total of 75 male DO mice (J:DO, JAX stock number 009376) from generation 35 were obtained from The Jackson Laboratory. All procedures involving these mice were approved by the University of North Carolina Institutional Animal Care and Use Committee. The study was limited to male mice to control for possible confounding effects of sex. The mice were all aged between 26 and 32 days upon receipt and were housed one per cage for the duration of the study. All mice were allowed to acclimate for 4 weeks before exposure to iAs under controlled conditions with a 12-h light/dark cycle at 22 ± 1 °C and 50 ± 10% relative humidity. During acclimatization, the mice were fed a semi-purified AIN-93G diet (Envigo Teklad, Madison, WI, USA) and drank As-free deionized water (DIW) ad libitum. In our previous studies, the concentration of iAs in the AIN-93G diet ranged from 11 to 50 ppb (Douillet et al. 2017; Huang et al. 2018a, b; Huang, et al. 2018a, b). The acclimatization allows for clearance of iAs to which the mice were exposed in The Jackson Laboratory while consuming a regular grain-based diet; this type of diet has been shown to contain up to 400 ppb As (Murko et al. 2018). After acclimatization, the 75 mice were switched to DIW containing sodium arsenite (NaAsO2, > 99% pure; Sigma-Aldrich, St. Louis, MO, USA) at final concentration of 100 μg As/L (100 ppb) for 26 weeks. This dose was selected because, based on a pharmacokinetic model developed by the US EPA, it was anticipated to yield total arsenic concentration in mouse livers consistent with that in human populations chronically exposed to the Maximum Contaminant Level for iAs in drinking water of 10 ppb (El-Masri and Kenyon 2008). Further, we have previously shown that this level of chronic iAs exposure induced T2D phenotypes in adult male C57BL/6 mice lacking the *As3mt* gene which, like humans, exhibit decreased capacity to metabolize iAs (Douillet et al. 2017). Water consumption was measured weekly, and food consumption was measured at the intervals shown in Fig. 1.

Metabolic phenotyping

Body weight and composition as well as seven T2D indicators were measured at selected time points before and during the exposure to iAs (Fig. 1).

Body weight and composition—Body weight was measured 13 times before and during the exposure as shown in Fig. 1. Body composition, including the percentages of body mass represented by fat (%fat) and by lean mass (%lean mass), was measured 2 weeks prior to iAs exposure (week-2) as well as in the middle and at the end of the exposure (weeks 12 and 24, respectively). The Echo MRI Three-in-one Composition Analyzer and Labmaster (Echo Medical Systems, Houston, TX, USA) was used for the body composition analysis.

Blood glucose and plasma insulin—Blood glucose and plasma insulin levels were measured both after 6-h of fasting and 15 min after intraperitoneal (i.p.) injection of glucose (2 g/kg bodyweight; Sigma-Aldrich) at 3–5 week intervals. Fasting blood glucose (FBG) and 15-min blood glucose (BG15) concentrations were measured by One Touch® Ultra® glucometer (LifeScan, Inc., Milpitas, CA). Sample preparations and glucose treatments were

always performed in the early afternoon, and were further organized such that the timing for each mouse was consistent over the course of the study. Plasma was isolated from blood by centrifugation at 1700×g for 15 min at 4 °C and stored at − 80 °C. Fasting plasma insulin (FPI) and 15-min plasma insulin (PI15) concentrations were measured using ELISA kits from Crystal Chem (Elk Grove Village, IL).

Homeostatic model assessment for β-cell function and insulin resistance (HOMA-B and HOMA-IR) and insulinogenic index—The homeostatic model assessment for β-cell function (HOMA-B), the homeostatic model assessment for insulin resistance (HOMA-IR), and insulinogenic index were calculated from the fasting and 15-min glucose and insulin concentrations using the following formulas:

$$\text{HOMA-B} = \frac{500 * FPI\left(\frac{\mu U}{mL}\right)}{\frac{FBG\left(\frac{mg}{dL}\right)}{18.2} - 3.5}$$

$$\text{HOMA-IR} = \frac{FBG\left(\frac{mg}{dL}\right) * FPI\left(\frac{\mu U}{mL}\right)}{16.2}$$

$$\text{Insulinogenic Index} = \frac{PI15\left(\frac{\mu U}{mL}\right) - FPI\left(\frac{\mu U}{mL}\right)}{0.04 * \left[BG15\left(\frac{\text{mg}}{\text{dL}}\right) - FBG\left(\frac{\text{mg}}{\text{dL}}\right)\right]}$$

Euthanasia and tissue collection

All mice were euthanized after 26 weeks of exposure to iAs by cervical dislocation. Tissues were collected after euthanasia, snap frozen, and stored at − 80 °C for future analyses.

Speciation analysis of As in urine and liver

We measured iAs and its metabolites both in livers and urine. The analysis of As species was carried out in spot urine samples (50–100 μl) collected immediately prior to iAs exposure (week – 2) and at the middle and end of exposure (weeks 12 and 24, respectively). Concentrations of iAs, MMAs, and DMAs were measured by hydride generationatomic absorption spectrometry coupled with a cryotrap using previously described procedures (Hernández-Zavala et al. 2008). The same method was used to measure concentrations of As species in 10% homogenates (w/v) prepared from livers collected after euthanasia. Both urine and liver homogenates were treated with 2% cysteine for 1 h prior to analysis to convert all pentavalent arsenicals to trivalency (Matoušek et al. 2008). The instrumental limits of detections (LODs) for iAs, MMAs, and DMAs using this method are 14, 8, and 20 pg As, respectively (Hernández-Zavala et al. 2008). These instrumental LODs translate to 0.28, 0.16, and 0.40 ppb in urine and 0.5–5.6, 0.4–3.2, and 1.0–8 ppb in liver, respectively, given the injected sample volumes and dilutions used in this study. In urine,

MMAs concentrations were below LOD for all samples, as were 31% ($n = 23$) of iAs concentrations. Conversely, DMAs concentrations in urine were all above LOD, as were all metabolite concentrations in livers. A value of zero was imputed for each value below LOD. The relative contributions of each As species in each tissue were then computed by dividing the concentration of each metabolite by the total arsenic concentration (tAs) in the tissue, which was calculated as the sum of the concentrations of iAs, MMAs, and DMAs. These proportions were then expressed as the percentage of tAs represented by iAs (%iAs), MMAs (%MMAs), or DMAs (%DMAs). While trimethyl arsine oxide has been detected in the urine of laboratory animals in some published studies (Waters et al. 2004), it was not detected in any of the urine samples analyzed in the current study.

Statistical analyses

The associations between iAs exposure and the final (week 25) value of each T2D indicator of interest were investigated using multiple linear regression. As mentioned above, the lack of genetic controls implied by using DO samples requires carefully controlling for potential confounding variables. Our approach was to specify a very large “full” model, and to eliminate variables by backwards selection that were not significant at the alpha = 0.1 level, always retaining iAs exposure and any main effects that were significant in interaction with other variables. To this end, in each regression, the full model controlled for cumulative iAs exposure (equivalently, the total amount of water consumed during exposure), the initial T2D indicator value, body weight, and adiposity (%fat), as well as all relevant two-way interactions.

Multiple linear regression was also employed to investigate the association between arsenic species present in liver with the week 25 T2D indicators. We employed the final reduced models that used cumulative iAs exposure as the independent variable as a starting point. Each term containing iAs exposure was replaced with three analogous terms: tAs concentration, %DMAs, and %MMAs in liver. We then applied a second round of backwards selection as above.

All models were fit using the lm() function in R (R Core Team 2020). Data visualizations were created using the ggplot2 (Wickham 2016) and ggcorrplot (Kassambara 2019) packages.

Results

Food and water consumption

The study design, including the timing of all T2D indicator measurements, is illustrated in Fig. 1. Although there was substantial inter-individual variability in weekly food consumption, the rates of food consumption (g/week) rose only modestly on average and for individual mice over the 30 week period (Figs. 2a & S1a); median consumption was 22.6 g/week (IQR: 21.3–24.2) immediately before iAs initiation (week 0) and 25.5 g/week (IQR: 23.2–26.9) at week 25; this difference was statistically significant ($p < 0.001$ by Wilcoxon Rank Sum test). Notwithstanding some week-to-week variability which was especially noticeable for mice with more extreme levels of consumption, we observed that the rates

of food consumption remained nearly constant after week 8. For most mice, weekly water consumption was even more constant over time (Figs. 2b & S1b), although there was even greater inter-individual variability, and a few extreme outliers. There are several examples of extreme week-to-week variability within samples that might be attributable to leaks in water bottles rather than true variability in consumption. Importantly, extreme consumption is correlated within mice over time. Water consumption was initially slightly elevated and decreased modestly during the first few weeks of the study, a pattern likely caused by the stress of acclimatization to a new environment. Median water consumption at week-2 was 24.0 g/week (IQR: 21.6–29.0) and decreased to 21.9 g/week (IQR: 18.9,26.2) at week 1, after which a slight linear increase was observed for the duration of follow-up: median consumption at week 26 was 27.1 g/week (IQR: 22.2–35.1). The difference from week-2 to week 26 was marginally significant ($p = 0.054$ by Wilcoxon Rank Sum Test).

Body weight and composition

The stability of food and water consumption over time is in marked contrast to the progression of body weight and composition (as measured by %fat) which increased significantly over the course of the study (Figs. 2c, d, S1c & d). The body weight gain was highest in the first half of the study after which it plateaued. Median body weight increased from 25.0 g (IQR: 23.3–27.4) at week-2 to 42.1 g (IQR 36.7–47.2) at week 24 and %fat more than doubled from 9.8% (IQR 6.7–13.6) to 23.4% (IQR 19.4–28.7). These differences were both highly significant ($p < 0.001$ by Wilcoxon Rank Sum test). Of note, notwithstanding minor fluctuations, the body weight trajectories appear nearly deterministic, increasing smoothly over time.

T2D indicators

The time courses for the T2D indicators were more variable, with substantial heterogeneity between mice and many outliers (Figs. 3 & S2). It was not uncommon for some mice to strongly deviate from the average trends. The distributions of the plasma insulin measures (FPI and PI15) became more skewed over time (Figs. 3a, b); the maximum FPI value increased from 6.2 to 78.8 ng/mL, while the maximum PI15 value increased from 5.9 to 39.7 ng/mL from week-1 to 25 (the extreme outlier at week 25 was the same sample for both measures). The median FPI at week-1 was 1.87 ng/mL (IQR: 1.30–2.70) compared to 3.37 ng/mL (IQR: 2.03–6.07) at week 25 ($p < 0.001$, by Wilcoxon rank sum test). The median PI15 at week −1 was 1.45 ng/mL (IQR: 1.08–2.04) compared to 3.49 ng/mL (IQR: 2.18–6.24) at week 25 ($p < 0.001$, by Wilcoxon rank sum test). By contrast, FBG decreased slightly over time, as shown in Figs. 3c & S2c. The median FBG at week-1 was 140.0 mg/dL (IQR: 121.5–159.0) compared to 122.5 mg/dL (IQR: 107.2–141.2) at week 25 ($p < 0.001$, by Wilcoxon rank sum test). BG15 did not change meaningfully over time, as illustrated in Figs. 3d & S2d ($p = 0.24$, by Wilcoxon rank sum test).

The distributions for the HOMA-B and HOMA-IR indices, which are derived from fasting glucose and insulin values, reveal the same pattern as seen for the insulin measurements (Figs. 3e, f, S2e & f): the maximum HOMA-B value increased from 823.8 to 13,932.5, while the maximum HOMA-IR value increased from 61.3 to. 554.3 from week-1 to 25 (again, the extreme outlier at week 25 for both measures came from the same sample as

for the FPI and PI15 measures). The median HOMA-B at week 3 was 236.17 (IQR: 164.73–338.44) compared to 551.4 (IQR: 248.5–1104.9) at week 25 ($p < 0.001$, by Wilcoxon rank sum test). The median HOMA-IR at week −1 was 15.30 (IQR: 10.17–23.90) compared to 23.80 (IQR: 15.00–46.35) at week 25 ($p < 0.001$, by Wilcoxon rank sum test). A very modest increase in insulinogenic index was observed, along with an increase in variability (Fig. 3g & S2g): the median value was − 0.05 (IQR: − 0.12, 0.02) at week-1 compared to 0.02 (IQR: − 0.10, 0.14) at week 25 ($p = 0.02$, by Wilcoxon rank sum test).

The correlations among the week 25 values of the seven T2D indicators are illustrated in Fig. 4. The two insulin indicators (FPI and PI15) are highly correlated. While still significant, the correlation between the two glucose indicators (FBG and BG15) is more modest. The salient feature of this correlogram is the strong correlations among the insulin indicators and three derived measurements; the insulin endpoints are highly positively correlated with HOMA-B and HOMA-IR and highly negatively correlated with insulinogenic index. Thus, the values of these indices are driven by plasma insulin, not blood glucose values.

Association between T2D indicators at week 25 and iAs exposure

The results of the model selection (i.e., which independent variables remained after the selection procedures) for each T2D indicator are summarized in Table 1. Log transformations were applied to the FPI and PI15 measurements to better achieve approximate normality of model residuals. A single outlier with extreme residual value was removed in the final models for FPI, HOMA-B, HOMA-IR, and insulinogenic index. A single sample was the outlier in the three derived indicators, while a unique sample was the outlier in the model for FPI. Removal of these outliers does not change the inference for the interaction terms, and in most cases makes it more conservative. The full models are included in Tables S1–S16 in online Appendix A, and the effect estimates that characterize the effect of iAs have been abstracted into Table 2 below. The salient result is that the association of cumulative iAs exposure in the FPI, PI15, HOMA-B, and HOMA-IR models manifested as significant interactions between iAs and body weight/composition. That is, each of these models contains a significant interaction between cumulative iAs exposure and either body weight or %fat. Because we scaled the independent variables in these models, the marginal effect of iAs exposure can be interpreted as the association between a one standard deviation increase in iAs exposure and the T2D indicator for mice of average body weight/composition. Although these marginal associations were somewhat paradoxically negative, they were not significant in any of the four models. The interaction effect (e.g., for log-transformed FPI) can be interpreted as follows: the effect of a one standard deviation increase in cumulative iAs exposure for mice with one standard deviation higher than average %fat (holding body weight constant) is − 0.16 + 0.29 = 0.13 ng/mL (Tables 1, 2 & S1). However, because these effects are best interpreted visually, we illustrate them as interaction plots in Fig. 5. The interaction plots visualize the predicted T2D indicator on the y-axes versus (standardized) iAs exposure on the x-axes, for the three quartiles of body weight/adiposity. The diabetogenic effect of iAs exposure at week 25 is only seen in mice in the highest quartile of %fat. Specifically, there is a positive slope for FPI, PI15, and HOMA-B for these mice. Although the slope remains negative for this quartile for

HOMA-IR, the salient pattern remains that the “protective” effect of iAs exposure in lower %fat quartiles attenuates and eventually reverses for larger/fatter mouse for all of these T2D indicators.

Body weight and/or adiposity was significantly associated with all T2D indicators except for FBG and insulinogenic index; both of these models were reduced until only iAs remained. While there was no significant relationship observed between iAs and FBG, a standard deviation increase was marginally associated with a 0.16 unit increase in insulinogenic index at week 25 ($p = 0.077$, Tables 1, 2 & S13). The only significant term in the model for BG15 other than the week-1 value was the interaction between weight and %fat: a simultaneous increase of one standard deviation in both body weight and %fat was associated with a 24.8 mg/dL decrease in BG15 at week 25 (Tables 1 & S8).

As noted above, there were several samples for which an elevated water consumption (at a single timepoint each) might be more accurately attributable to leaking water bottles than to true week-to-week variability in water consumption. We conducted sensitivity analyses in which we replaced these suspect consumption values by linearly interpolating between the consumptions at the two time points immediately adjacent. We re-ran the models for the four T2D surrogates with significant interaction effects; the parameter estimates and inference were nearly identical in all cases.

Association between liver arsenic species and T2D indicators at week 25

The final (log-transformed) FPI models using the liver arsenic species as independent variables are included in Tables S3 & 4. Notably, the significant interaction between cumulative iAs exposure and adiposity in the model for FPI is replaced with an analogous significant interaction between the proportion of DMAs (%DMAs) and adiposity; this interaction is visualized in Fig. 6. Similarly, the proportion of DMAs replaces cumulative iAs exposure in the significant association with HOMA-IR (Tables S15 & S16, online Appendix A); on average, a ten percent increase in DMAs is associated with a nearly 94 unit increase in insulinogenic index. These were the only T2D indicators to exhibit significant associations with liver arsenic species. When the significant liver species terms were replaced with their analogous 24-week urine species terms, these associations were not significant.

Discussion

DO mice are an established model to study gene–environment interactions and genetic susceptibility to adverse effects of environmental exposures observed in human populations. Inorganic arsenic has been classified as an environmental diabetogen (Maull et al. 2012), and the diabetogenic effects of iAs exposure have been shown to vary among individuals and human populations, depending in part on the efficiency of iAs detoxification via the AS3MT-catalyzed methylation pathway and on AS3MT polymorphism (Drobná et al. 2013; Kuo et al. 2017). The present study was designed to characterize the inter-individual differences in indicators of obesity and T2D in the genetically diverse DO mice exposed to iAs, and to our knowledge is the first study to do so. The DO are well suited to this purpose, as they have been shown to exhibit a wide range of phenotypic variability in response

to many different types of experimental exposures (French et al. 2015; Kurtz et al. 2020; Mayeux et al. 2018; Patterson et al. 2020; Recla et al. 2019); they were similarly expected to exhibit an expanded range of variability for the iAs-induced T2D indicators of interest and in their capacities to metabolize iAs compared to existing inbred lines. These indicators were assessed in the DO mice before and during a 26-week period of chronic iAs exposure. Two striking findings are reported here. First, a broad variation was observed among the DO mice in obesity and T2D indicators when exposed to iAs. Second, an interactive effect between body weight and/or adiposity and iAs exposure was identified in relation to the assessed T2D indicators. Specifically, mice that were obese and exposed to iAs displayed significant positive trends in T2D indicators.

The DO mice exhibited large inter-individual variation in body weight, food, and water consumption. For example, at week 30, the largest mouse was more than twice size of smallest (57.7 g vs 26.5 g, respectively). Similarly, while weekly water consumption after week 11 was more or less constant for individual mice, the range of consumption varied almost fivefold (e.g., 16.1 to 80.4 g/week) across the DO population.

We observed significant interactions between cumulative iAs exposure and body weight or adiposity for the FPI, PI15, HOMA-B, and HOMA-IR measures. While for mice of average body weight (or %fat) the association was paradoxically (though mostly insignificantly) protective, for large (or obese) mice diabetogenic effects of iAs exposure were apparent and were consistent with insulin resistance. Similarly, we observed an analogous interaction between the proportion of DMAs present in the liver and adiposity on FPI. While obesity is known to modify iAs metabolism in humans (Lin et al. 2014; Lindberg et al. 2007; Su et al. 2012), to our knowledge, these interactions constitute novel associations in experimental mouse models like the DO.

The present study contributes to a growing body of research documenting the complex associations between iAs and its metabolites and T2D and its indicators. The interactions we observed are consistent with recent evidence from a human population in Chile, in which the increase in the odds of T2D associated with iAs exposure from drinking water was higher among obese subjects compared to lean subjects (Castriota et al. 2018). Further, a recent analysis of NHANES data documented a nonlinear association between urinary DMAs and BMI (Warwick et al. 2021). The confluence of these lines of research highlights the need for more studies in experimental populations to better understand and quantify these complex associations.

Although we have uncovered a significant interactive effect between iAs and obesity in the context of T2D indicators, our study is not without limitations. For example, studies using DO mice necessarily preclude inclusion of genetically matched controls, since each mouse is genetically unique. The study design we employed therefore mimicked that of an exposed human population, where the genetic diversity of the mice provides the variation in response, in contrast to a design that includes untreated mice. This lack of a control group requires carefully controlling for possible confounding variables, which motivated us to adopt a statistical approach common in population studies and other non-randomized datasets where inclusion of such control groups is often not possible. One might expect

the overall genetic contributions of NOD and NZO to the DO sample genomes to be two such confounders, since these strains were themselves bred to be models of type I diabetes and obesity, respectively (Noll et al. 2019). That is, a potential concern is that imbalances in these founder contributions could confound our observed relationships, if these founder contributions are associated with the diabetes outcomes of interest. Although we did not include these founder contributions in our statistical models, we did not anticipate them to be confounders in the DO, since NOD and NZO are highly polygenic models which likely manifest their extreme outcomes in inbred strains due to the combined recessive and epistatic effects at a large number of loci, which would not be the case in an outbred population like the DO. After genotyping our samples, we formally tested and confirmed this logic (online Appendix B). The fact that we studied only male mice is another limitation, but one that came with a concurrent benefit. While we are aware that sex might modify the effect of iAs exposure in mice (Douillet et al. 2017; Drobna et al. 2009), in restricting our study to male samples only, we also deliberately eliminated the possible confounding effect of sex. A further limitation of this work is the possible lack of generalizability to human populations as mice are known to metabolize iAs far more efficiently than humans (Vahter 1999). This point is illustrated in the ternary plots in Fig. 7. Figure 7a displays the distribution of the observed arsenic species present in the urine collected immediately prior to sacrifice (week 24), and Fig. 7b shows the distribution of arsenic species present in the liver samples collected at sacrifice. As shown, these compositions are dominated by DMAs, while there is very little contribution of MMAs (in the case of the urine samples, all had MMAs measured below the LOD). This is in marked contrast to the distributions observed in the urine of humans that have been chronically exposed to iAs. For example, the relative contributions of iAs and MMAs were 4.4–37.9% and 5.9–29.3%, respectively, in one U.S. population chronically exposed to iAs in drinking water (Hudgens et al. 2016).

The relative contributions of the observed As species that we have documented in our small cohort of DO mice are similar to those that have been documented in inbred strains, including the Collaborative Cross (CC) (Douillet et al. 2017; Huang et al. 2018a, b; Stýblo et al. 2019). This extremely efficient metabolization has motivated a recently published humanized *AS3MT* mouse model, which was created to metabolize iAs in a manner much more similar to humans (Koller et al. 2020). We are currently employing this model to create diverse congenic CC lines that carry this humanized version of *AS3MT*, which should serve as an ideal resource for further studying the significant interactions that we have observed in the current study, as their iAs metabolization profiles should mimic that seen in the human population. Further, we intentionally selected CC strains to be recipients of the humanized *AS3MT* gene that manifest extremes of obesity from among the extant CC strains to maximize their relevance to the study of T2D. These lines will also be fully reproducible, thus allowing for the inclusion of genetic case-controls, and thus the ability to infer causal genetic effects.

Supplementary Material

Refer to Web version on PubMed Central for supplementary material.

Funding

This study was funded by the National Institute of Environmental Health Sciences grants R01ES029925 to R.C.F., F.P.M.D.V., and M.S. and R01ES028721 to M.S. and R.C.F., and by the UNC Superfund Research Program Grant P42ES031007. Additional support was provided by the UNC Institute for Environmental Health Solutions and the UNC Nutrition Obesity Research Center grant DK056350 from National Institute of Diabetes and Digestive and Kidney Diseases. J.G.X. is funded by training grant T32ES007126.

Data Availability

All data from this study have been deposited in the Mouse Phenome Database (https://phenome.jax.org/projects/Xenakis2).

References

Agency for Toxic Substances and Disease Registry (ATSDR) (2007) Toxicological profile for Arsenic. U.S. Department of Health and Human Services, Public Health Service, Atlanta, GA. 10.15620/cdc:11481

Agusa T, Fujihara J, Takeshita H, Iwata H (2011) Individual variations in inorganic arsenic metabolism associated with AS3MT genetic polymorphisms. Int J Mol Sci 12(4):2351–2382. 10.3390/ijms12042351 [PubMed: 21731446]

Babu DA, Deering TG, Mirmira RG (2007) A feat of metabolic proportions: Pdx1 orchestrates islet development and function in the maintenance of glucose homeostasis. Mol Genet Metab 92(1–2):43–55. 10.1016/j.ymgme.2007.06.008 [PubMed: 17659992]

Castriota F, Acevedo J, Ferreccio C, Smith AH, Liaw J, Smith MT, Steinmaus C (2018) Obesity and increased susceptibility to arsenic-related type 2 diabetes in Northern Chile. Environ Res 167:248–254. 10.1016/j.envres.2018.07.022 [PubMed: 30059859]

Castriota F, Rieswijk L, Dahlberg S, La Merrill MA, Steinmaus C, Smith MT, Wang JC (2020) A state-of-the-science review of arsenic's effects on glucose homeostasis in experimental models. Environ Health Perspect 128(1):016001. 10.1289/EHP4517 [PubMed: 31898917]

CDC. 2020. National Diabetes Statistics Report (2020) | CDC. https://www.cdc.gov/diabetes/data/statistics-report/index.html. Accessed 10 Aug 2021

Chesler EJ, Gatti DM, Morgan AP, Strobel M, Trepanier L, Oberbeck D, McWeeney S, Hitzemann R, Ferris M, McMullan R, Clayshultle A, Bell TA, Manuel de Villena FP, Churchill GA (2016) Diversity outbred mice at maintaining allelic variation in the face of selection. G3 6(12):3893–3902. 10.1534/g3.116.035527 [PubMed: 27694113]

Churchill GA, Gatti DM, Munger SC, Svenson KL (2012) The diversity outbred mouse population. Mammalian Genome 23(9–10):713–718. 10.1007/s00335-012-9414-2 [PubMed: 22892839]

Cubadda F, Jackson BP, Cottingham KL, Horne YOV, Kurzius-Spencer M (2017) Human exposure to dietary inorganic arsenic and other arsenic species: state of knowledge, gaps and uncertainties. Sci Total Environ 579:1228–1239. 10.1016/j.scitotenv.2016.11.108 [PubMed: 27914647]

Douillet C, Huang MC, Jesse Saunders R, Dover EN, Zhang C, Stýblo M (2017) Knockout of arsenic (+3 Oxidation State) methyltransferase is associated with adverse metabolic phenotype in mice: the role of sex and arsenic exposure. Arch Toxicol 91(7):2617–2627. 10.1007/s00204-016-1890-9 [PubMed: 27847981]

Douillet C, Ji J, Meenakshi IL, Lu K, de Villena FP, Fry RC, Stýblo M (2021) Diverse genetic backgrounds play a prominent role in the metabolic phenotype of CC021/Unc and CC027/GeniUNC mice exposed to inorganic arsenic. Toxicology 452:152696. 10.1016/j.tox.2021.152696 [PubMed: 33524430]

Drobna Z, Naranmandura H, Kubachka KM, Edwards BC, Herbin-Davis K, Miroslav Styblo X, Le C, Creed JT, Maeda N, Hughes MF, Thomas DJ (2009) Disruption of the Arsenic (+3 Oxidation State) methyltransferase gene in the mouse alters the phenotype for methylation of arsenic and affects distribution and retention of orally administered arsenate. Chem Res Toxicol 22(10):1713–1720. 10.1021/tx900179r [PubMed: 19691357]

Drobná Z, Del Razo LM, García-Vargas GG, Sánchez-Peña LC, Barrera-Hernández A, Stýblo M, Loomis D (2013) Environmental exposure to arsenic, AS3MT polymorphism and prevalence of diabetes in Mexico. J Eposure Sci Environ Epidemiol 23(2):151–155. 10.1038/jes.2012.103

El-Masri HA, Kenyon EM (2008) Development of a human physiologically based pharmacokinetic (PBPK) model for inorganic arsenic and its mono- and di-methylated metabolites. J Pharmacokinet Pharmacodyn 35(1):31–68. 10.1007/s10928-007-9075-z [PubMed: 17943421]

French JE, Gatti DM, Morgan DL, Kissling GE, Shockley KR, Knudsen GA, Shepard KG, Price HC, King D, Witt KL, Pedersen LC, Munger SC, Svenson KL, Churchill GA (2015) Diversity outbred mice identify population-based exposure thresholds and genetic factors that influence benzene-induced genotoxicity. Environ Health Perspect 123(3):237–245. 10.1289/ehp.1408202 [PubMed: 25376053]

Fujimoto K, Polonsky KS (2009) Pdx1 and other factors that regulate pancreatic β-Cell survival. Diabetes Obes Metab 11:30–37. 10.1111/j.1463-1326.2009.01121.x [PubMed: 19817786]

Harrill AH, Borghoff S, Zorrilla L, Blystone C, Kissling GE, Malarkey D, Shockley K, Travlos G, DeVito MJ (2018) NTP research report on baseline characteristics of diversity outbred (J:DO) mice relevant to toxicology studies. NTP Res Rep. 10.22427/NTP-RR-6

Heindel JJ, Blumberg B, Cave M, Machtinger R, Mantovani A, Men-dez MA, Nadal A, Palanza P, Panzica G, Sargis R, Vandenberg LN, vom Saal F (2017) Metabolism disrupting chemicals and metabolic disorders. Reprod Toxicol 68:3–33. 10.1016/j.reprotox.2016.10.001 [PubMed: 27760374]

Hernández-Zavala A, Matoušek T, Drobná Z, Paul DS, Walton F, Adair BM, Dědina J, Thomas DJ, Stýblo M (2008) Speciation analysis of arsenic in biological matrices by automated hydride generation-cryotrapping-atomic absorption spectrometry with multiple microflame quartz tube atomizer (Multiatomizer). J Anal at Spectrom 23(3):342–351. 10.1039/B706144G [PubMed: 18677417]

Huang MC, Douillet C, Dover EN, Stýblo M (2018a) Prenatal arsenic exposure and dietary folate and methylcobalamin supplementation alter the metabolic phenotype of C57BL/6J mice in a sex-specific manner. Arch Toxicol 92(6):1925–1937. 10.1007/s00204-018-2206-z [PubMed: 29721587]

Huang MC, Douillet C, Dover EN, Zhang C, Beck R, Tejan-Sie A, Krupenko SA, Stýblo M (2018b) Metabolic phenotype of wild-type and as3mt-Knockout C57BL/6J mice exposed to inorganic arsenic: the role of dietary fat and folate intake. Environ Health Perspect 126(12):127003. 10.1289/EHP3951 [PubMed: 30675811]

Hudgens EE, Drobna Z, Le Bin He XC, Styblo M, Rogers J, Thomas DJ (2016) Biological and behavioral factors modify urinary arsenic metabolic profiles in a U.S. population. Environmental Health 15:62. 10.1186/s12940-016-0144-x [PubMed: 27230915]

IARC (2004) Some Drinking-Water Disinfectants and Contaminants, Including Arsenic

Kassambara A (2019) Ggcorrplot: Visualization of a Correlation Matrix Using Ggplot2

Keele GR, Zhang T, Pham DT, Vincent M, Bell TA, Hock P, Shaw GD, Munger SC, de Villena FPM, Ferris MT, Gygi SP, Churchill GA (2020) Regulation of protein abundance in genetically diverse mouse populations. Cell Genom. 10.1101/2020.09.18.296657

Koller BH, Snouwaert JN, Douillet C, Jania LA, El-Masri H, Thomas DJ, Stýblo M (2020) Arsenic metabolism in mice carrying a *BORCS7/AS3MT* locus humanized by syntenic replacement. Environ Health Perspect 128(8):087003. 10.1289/EHP6943 [PubMed: 32779937]

Kuo C-C, Moon K, Thayer KA, Navas-Acien A (2013) Environmental chemicals and Type 2 diabetes: an updated systematic review of the epidemiologic evidence. Curr DiabRep 13(6):831–849. 10.1007/s11892-013-0432-6

Kuo C-C, Moon KA, Wang S-L, Silbergeld E, Navas-Acien A (2017) The association of arsenic metabolism with cancer, cardiovascular disease, and diabetes: a systematic review of the epidemiological evidence. Environ Health Perspect 125(8):087001. 10.1289/EHP577 [PubMed: 28796632]

Kurtz SL, Rossi AP, Beamer GL, Gatti DM, Kramnik I, Elkins KL (2020) “The diversity outbred mouse population is an improved animal model of vaccination against tuberculosis that reflects heterogeneity of protection” edited by Stallings CL. MSphere. 10.1128/mSphere.00097-20

Lin H-C, Huang Y-K, Shiue H-S, Chen L-S, Choy C-S, Huang S-R, Han B-C, Hsueh Y-M (2014) Arsenic methylation capacity and obesity are associated with insulin resistance in obese children and adolescents. Food Chem Toxicol 74:60–67. 10.1016/j.fct.2014.08.018 [PubMed: 25241017]

Lindberg A-L, Kumar R, Goessler W, Thirumaran R, Gurzau E, Koppova K, Rudnai P, Leonardi G, Fletcher T, Vahter M (2007) Metabolism of low-dose inorganic arsenic in a central european population: influence of sex and genetic polymorphisms. Environ Health Perspect 115(7):1081–1086. 10.1289/ehp.10026 [PubMed: 17637926]

Logan RW, Robledo RF, Recla JM, Philip VM, Bubier JA, Jay JJ, Harwood C, Wilcox T, Gatti DM, Bult CJ, Churchill GA, Chesler EJ (2013) High-precision genetic mapping of behavioral traits in the diversity outbred mouse population. Genes Brain Behav 12(4):424–437. 10.1111/gbb.12029 [PubMed: 23433259]

Martin EM, Stýblo M, Fry RC (2017) Genetic and epigenetic mechanisms underlying arsenic-associated diabetes mellitus: a perspective of the current evidence. Epigenomics 9(5):701–710. 10.2217/epi-2016-0097 [PubMed: 28470093]

Matoušek T, Hernández-Zavala A, Svoboda M, Langrová L, Adair BM, Drobná Z, Thomas DJ, Stýblo M, Dědina J (2008) Oxidation state specific generation of arsines from methylated arsenicals based on L-Cysteine treatment in buffered media for speciation analysis by hydride generation-automated cryotrapping-gas chromatography-atomic absorption spectrometry with the multiatomizer. Spectrochim Acta Part B 63(3):396–406. 10.1016/j.sab.2007.11.037

Maull EA, Ahsan H, Edwards J, Longnecker MP, Navas-Acien A, Pi J, Silbergeld EK, Styblo M, Tseng CH, Thayer KA, Loomis D (2012) Evaluation of the association between arsenic and diabetes: a national toxicology program workshop review. Environ Health Perspect 120(12):1658–1670. 10.1289/ehp.1104579 [PubMed: 22889723]

Mayer-Davis EJ, Lawrence JM, Dabelea D, Divers J, Isom S, Dolan L, Imperatore G, Linder B, Marcovina S, Pettitt DJ, Pihoker C, Saydah S, Wagenknecht L (2017) Incidence trends of Type 1 and Type 2 diabetes among youths, 2002–2012. N Engl J Med 376(15):1419–1429. 10.1056/NEJMoa1610187 [PubMed: 28402773]

Mayeux JM, Escalante GM, Christy JM, Pawar RD, Kono DH, Pollard KM (2018) Silicosis and silica-induced autoimmunity in the diversity outbred mouse. Front Immunol. 10.3389/fimmu.2018.00874

Murko M, Elek B, Styblo M, Thomas DJ, Francesconi KA (2018) Dose and diet—sources of arsenic intake in mouse in utero exposure scenarios. Chem Res Toxicol 31(2):156–164. 10.1021/acs.chemrestox.7b00309 [PubMed: 29244955]

Noll KE, Ferris MT, Heise MT (2019) The collaborative cross: a systems genetics resource for studying host-pathogen interactions. Cell Host Microbe 25(4):484–498. 10.1016/j.chom.2019.03.009 [PubMed: 30974083]

Patterson AM, Artur Plett P, Chua HL, Sampson CH, Fisher A, Feng H, Unthank JL, Miller SJ, Katz BP, MacVittie TJ, Orschell CM (2020) Development of a model of the acute and delayed effects of high dose radiation exposure in jackson diversity outbred mice; comparison to inbred C57BL/6 mice. Health Phys 119(5):633–646. 10.1097/HP.0000000000001344 [PubMed: 32932286]

R Core Team (2020) R: A Language and Environment for Statistical Computing. Vienna, Austria.: R Foundation for Statistical Computing

Recla JM, Bubier JA, Gatti DM, Ryan JL, Long KH, Robledo RF, Glidden NC, Hou G, Churchill GA, Maser RS, Zhang Z-W, Young EE, Chesler EJ, Bult CJ (2019) Genetic mapping in diversity outbred mice identifies a Trpa1 variant influencing late-phase formalin response. Pain 160(8):1740–1753. 10.1097/j.pain.0000000000001571 [PubMed: 31335644]

Roglic G, Organization WH (eds) (2016) Global report on diabetes. World Health Organization, Geneva

Stanton BA, Caldwell K, Congdon CB, Disney J, Donahue M, Ferguson E, Flemings E, Golden M, Guerinot ML, Highman J, James K, Carol Kim R, Lantz C, Marvinney RG, Mayer G, Miller D, Ana Navas-Acien D, Nordstrom K, Postema S, Rardin L, Rosen B, SenGupta A, Shaw J, Stanton E, Susca P (2015) MDI biological laboratory arsenic summit: approaches to limiting human exposure to arsenic. Curr Environ Health Rep 2(3):329–337. 10.1007/s40572-015-0057-9 [PubMed: 26231509]

St-Onge MP, Janssen I, Heymsfield SB (2004) Metabolic syndrome in normal-weight americans: new definition of the metabolically obese, normal-weight individual. Diabetes Care 27(9):2222–2228. 10.2337/diacare.27.9.2222 [PubMed: 15333488]

Stýblo M, Douillet C, Bangma J, Eaves LA, de Villena FP, Fry R (2019) Differential metabolism of inorganic arsenic in mice from genetically diverse collaborative cross strains. Arch Toxicol 93(10):2811–22. 10.1007/s00204-019-02559-7 [PubMed: 31493028]

Su C-T, Lin H-C, Choy C-S, Huang Y-K, Huang S-R, Hsueh Y-M (2012) The relationship between obesity, insulin and arsenic methylation capability in Taiwan adolescents. Sci Total Environ 414:152–158. 10.1016/j.scitotenv.2011.10.023 [PubMed: 22104380]

Sumi D, Himeno S (2012) Role of arsenic (+3 Oxidation State) methyltransferase in arsenic metabolism and toxicity. Biol Pharm Bull 35(11):1870–1875. 10.1248/bpb.b212015 [PubMed: 23123458]

Svenson KL, Gatti DM, Valdar W, Welsh CE, Cheng R, Chesler EJ, Palmer AA, McMillan L, Churchill GA (2012) High-resolution genetic mapping using the mouse diversity outbred population. Genetics 190(2):437–447. 10.1534/genetics.111.132597 [PubMed: 22345611]

Vahter M (1999) Methylation of inorganic arsenic in different mammalian species and population groups. Sci Prog 82(Pt 1):69–88. 10.1177/003685049908200104 [PubMed: 10445007]

Warwick M, Marcelo C, Marcelo C, Shaw J, Qayyum R (2021) The Relationship between chronic arsenic exposure and body measures among US adults: national health and nutrition examination survey 2009–2016. J Trace Elem Med Biol 67:126771. 10.1016/j.jtemb.2021.126771 [PubMed: 33991841]

Waters SB, Devesa V, Fricke MW, Creed JT, Stýblo M, Thomas DJ (2004) Glutathione modulates recombinant rat arsenic (+3 Oxidation State) methyltransferase-catalyzed formation of trimethylarsine oxide and trimethylarsine. Chem Res Toxicol 17(12):1621–1629. 10.1021/tx0497853 [PubMed: 15606138]

Wickham H (2016) Ggplot2: elegant graphics for data analysis. Springer-Verlag, New York

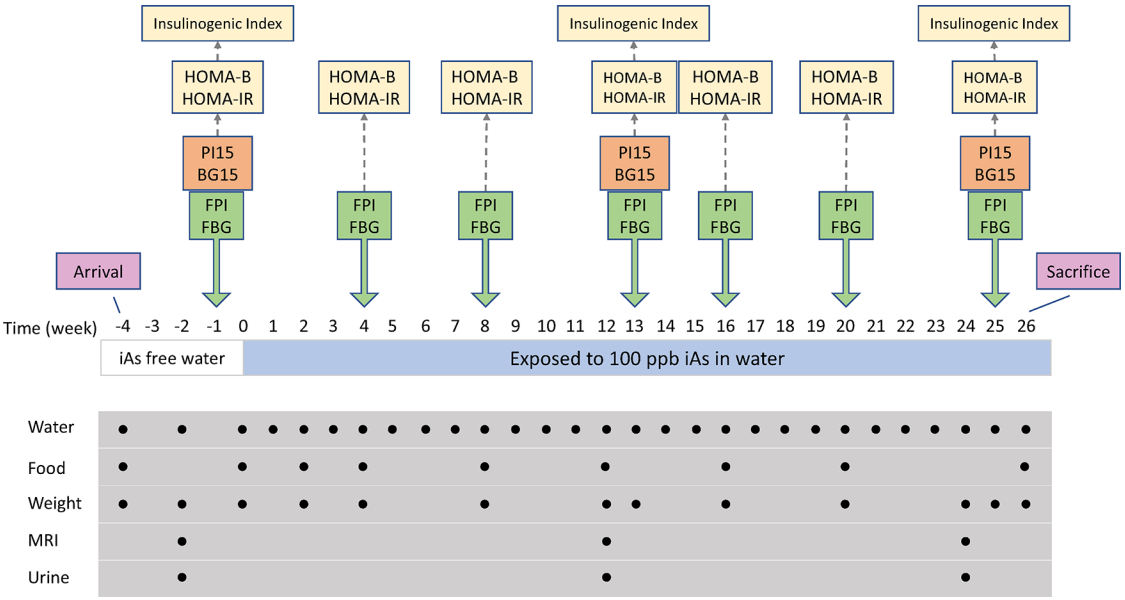

Fig. 1.

Study design. Metabolic phenotypes measured are displayed above the relevant measurement occasions (yellow indicates derived phenotypes). Administration and measurement of water and food consumed as well as measurement of body weight were conducted at regular timepoints indicated below weekly time series (mice were given arsenic-free water for frst four weeks, after which arsenic was introduced to the water). Body composition by MRI and urine collection were performed at weeks – 2, 12, and 24

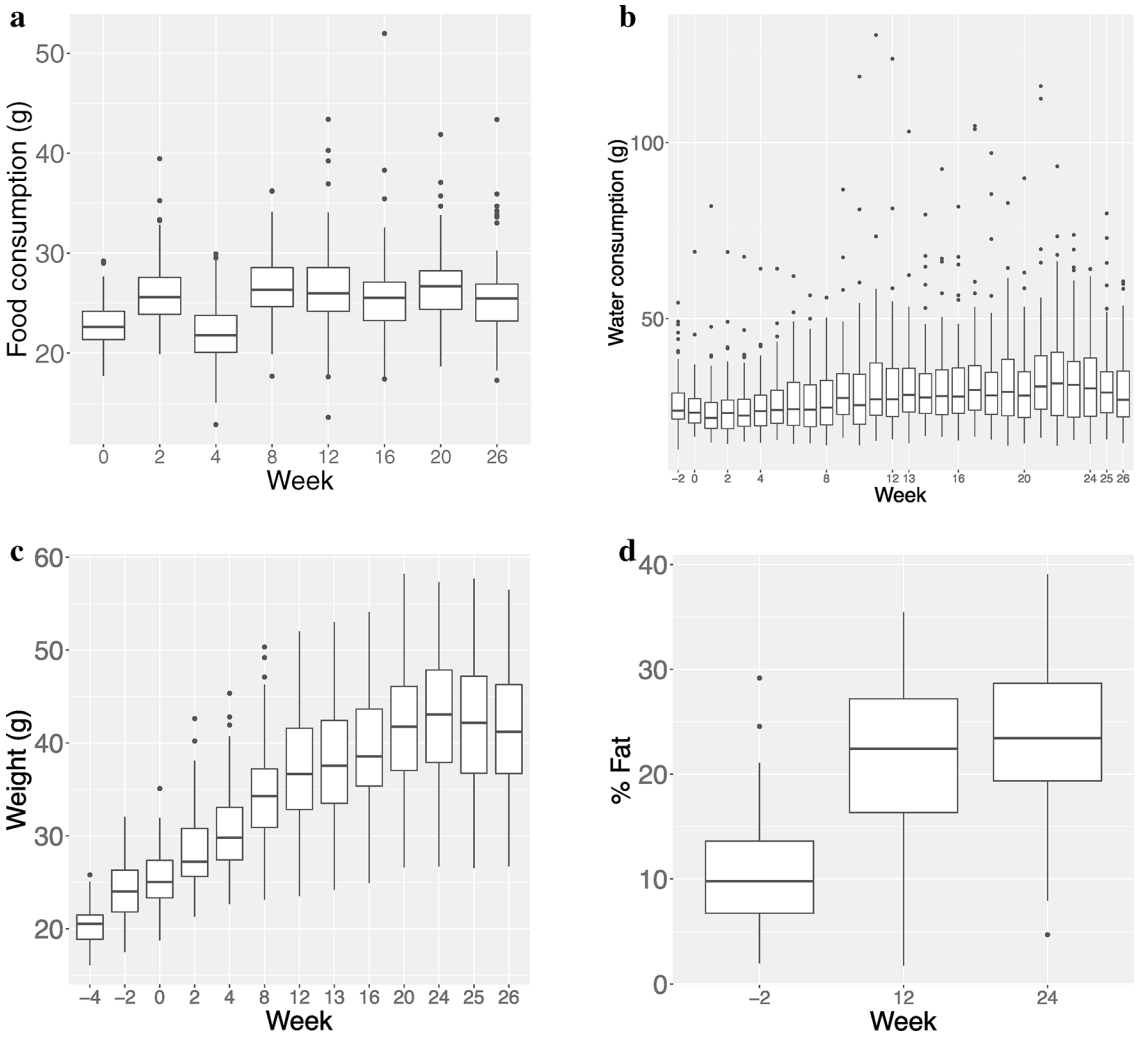

Fig. 2.

Box and whisker plots of food consumption, water consumption, body weight and %fat over time; **a** Food consumption over time. Rate of food consumption remains nearly constant after week 8; **b** Water consumption over time. Elevated initial consumption is likely associated with acclimatization to new environment; after an initial drop, consumption remains nearly constant for almost all mice; **c** Body weight over time. Body weight increased quickly during first half of study, followed by a plateau in the second half; **d** %fat over time. Body fat increases quadratically, remaining fairly constant in later weeks

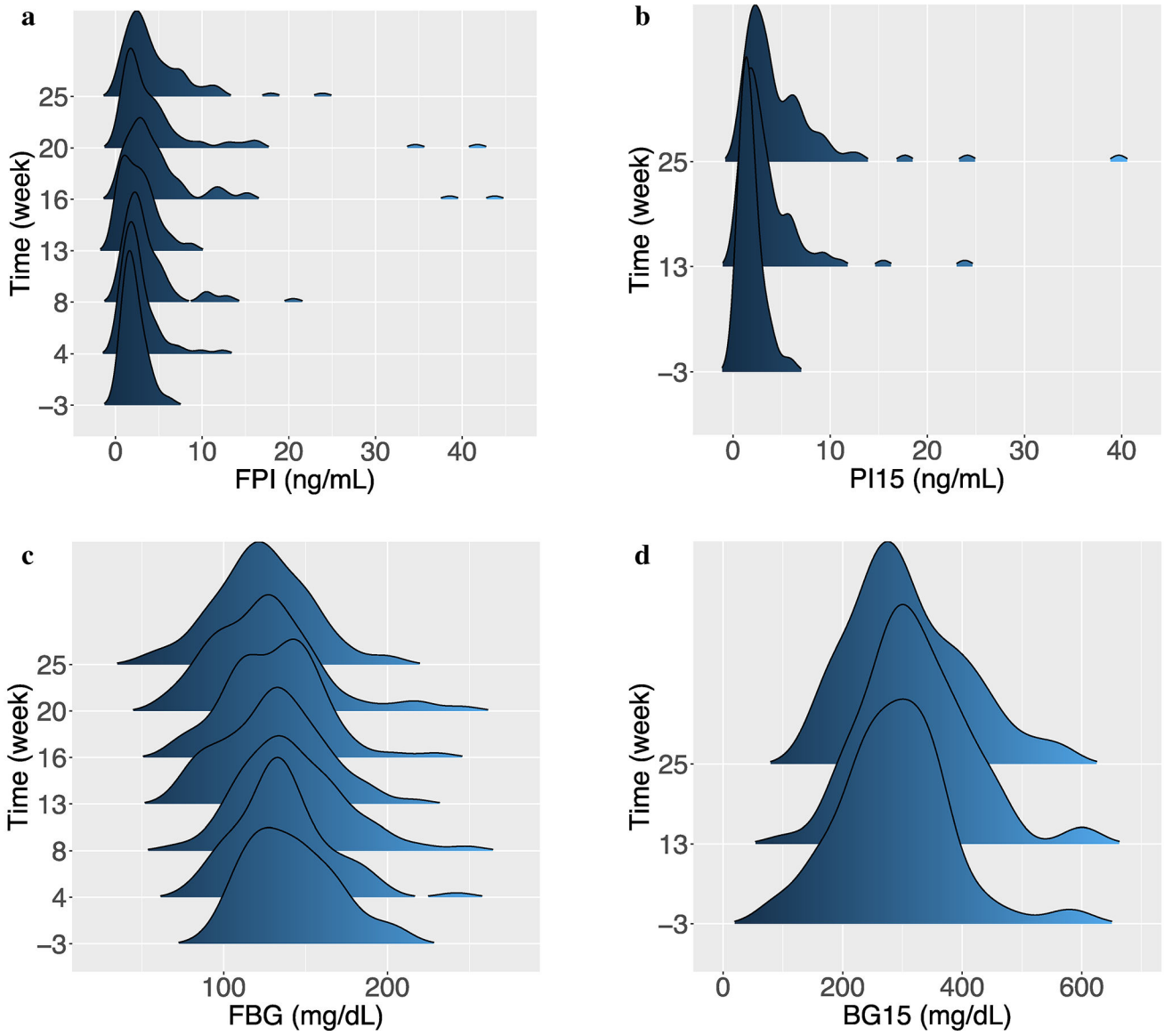

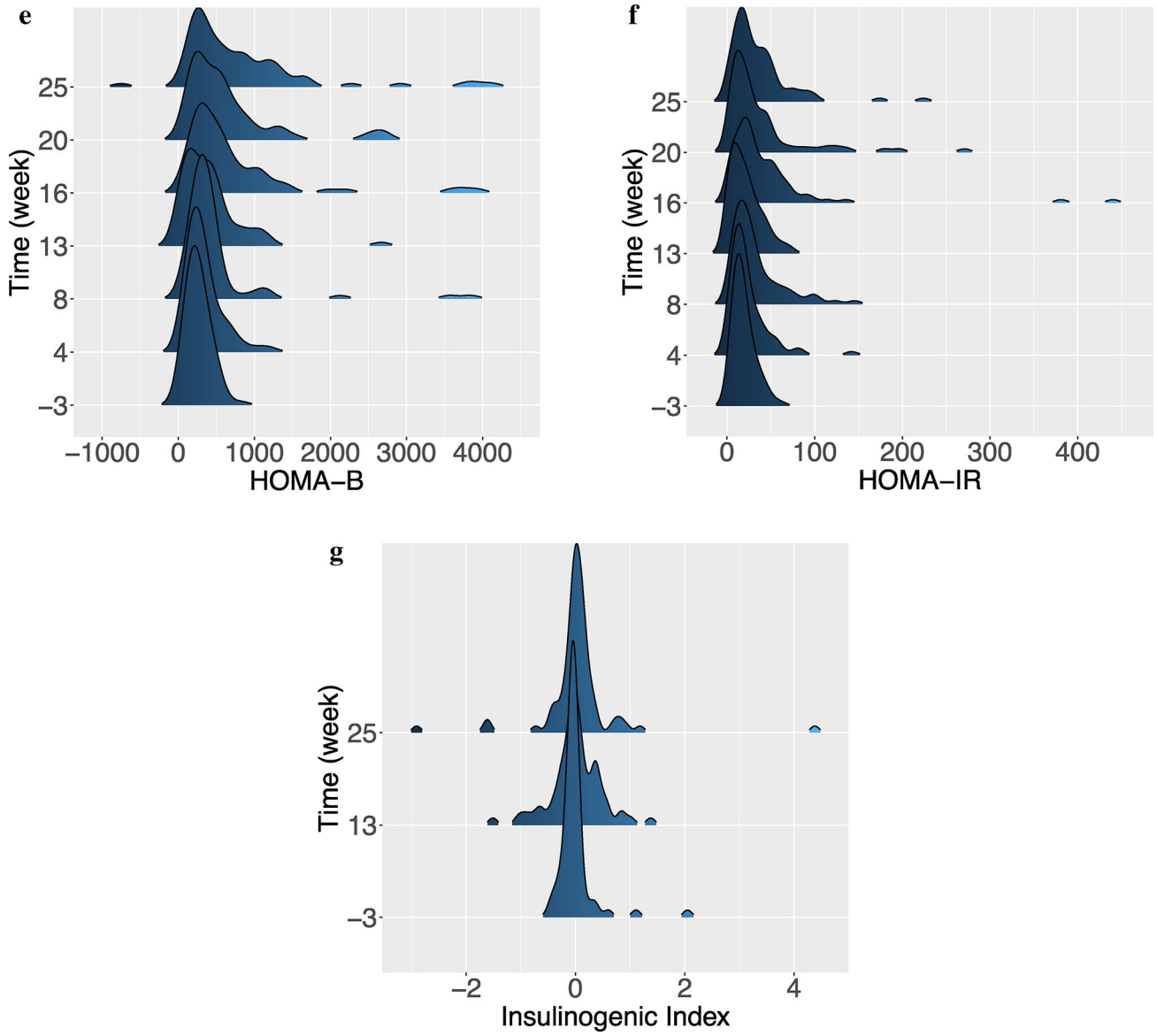

Fig. 3.

Metabolic phenotyping over time; **a** Distribution of FPI over time. One outlier with a value of 78.9 ng/mL was removed for the purposes of visualization; **b** Distribution of PI15 over time; **c** Distribution of FBG over time; **d** Distribution of BG15 over time; **e** Distribution of HOMA-B over time. Two outliers with values of 4880.6 and 13,932.5 were removed for improved visualization; **f** Distribution of HOMA-IR over time. One outlier with a value of 554.3 was removed for improved visualization; **g** Distribution of insulinogenic index over time. One outlier with a value of −26.4 was removed for improved visualization

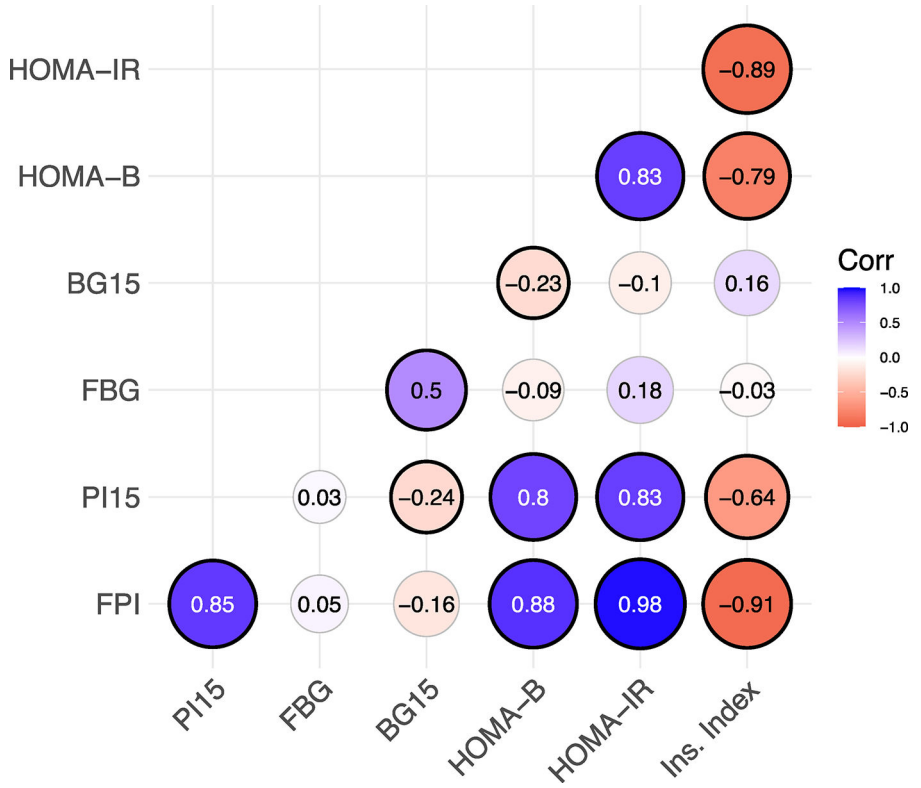

Fig. 4.

Correlogram of metabolic indicators at week 25. The size of each circle is directly proportional to the magnitude of the Spearman correlation coefcient, which is annotated at the center of each circle. Black outlines indicate signifcance at the alpha=0.05 level. Insulin phenotypes are highly correlated with each other, and with the derived phenotypes (HOMA-B, HOMA-IR and insulinogenic index)

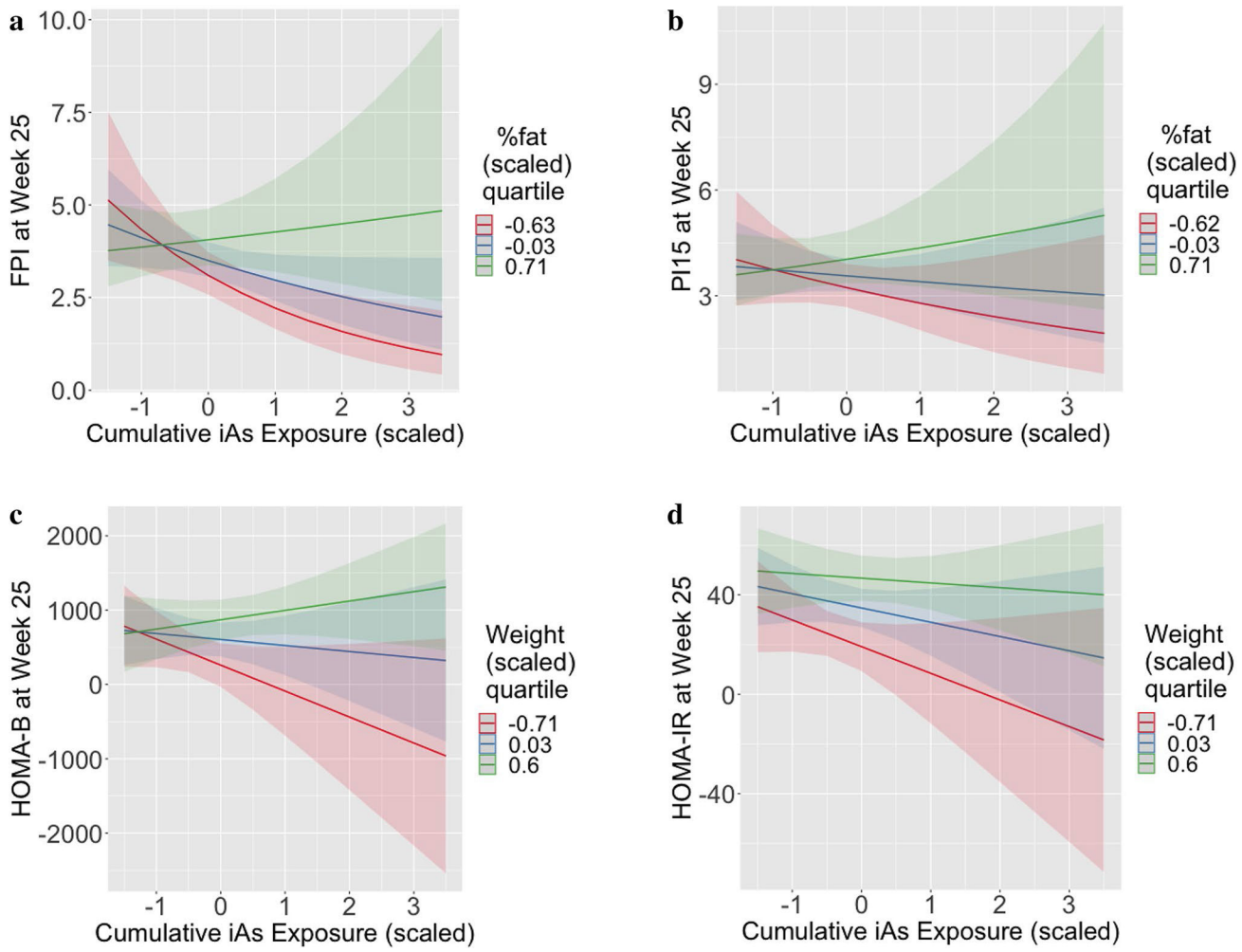

Fig. 5.

Visualization of interaction effects for insulin phenotypes from multiple linear regressions; **a** Prediction of FPI at week 25 as a function of cumulative iAs consumption, at three quartiles of body fat percentage (Q1=red, median=blue, Q3=green). Bands indicate 95% CI; **b** Prediction of PI15 at week 25 as a function of cumulative iAs consumption, at three quartiles of body fat percentage (Q1=red, median=blue, Q3=green). Bands indicate 95% CI; **c** Prediction of HOMA-B at week 25 as a function of cumulative iAs consumption, at three quartiles of body weight (Q1=red, median=blue, Q3=green). Bands indicate 95% CI; **d** Prediction of HOMA-IR at week 25 as a function of cumulative iAs consumption, at three quartiles of body weight (Q1=red, median=blue, Q3=green). Bands indicate 95% CI

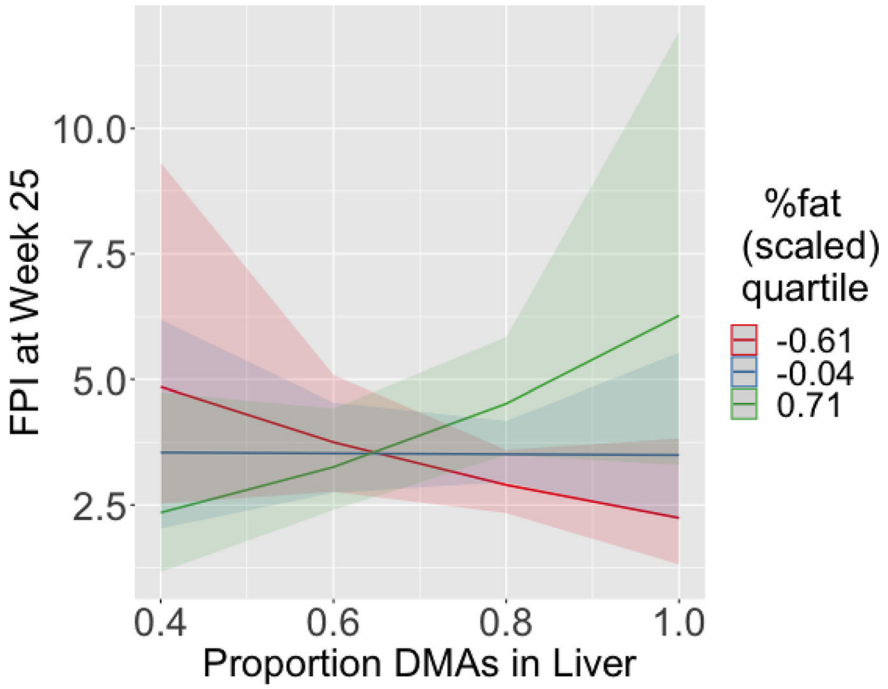

Fig. 6.

Visualization of interaction effects for prediction of FPI at week 25 from multiple linear regressions using liver arsenic species as independent variables as a function of cumulative iAs consumption, at three quartiles of body fat percentage (Q1 = red, median = blue, Q3 = green). Bands indicate 95% CI

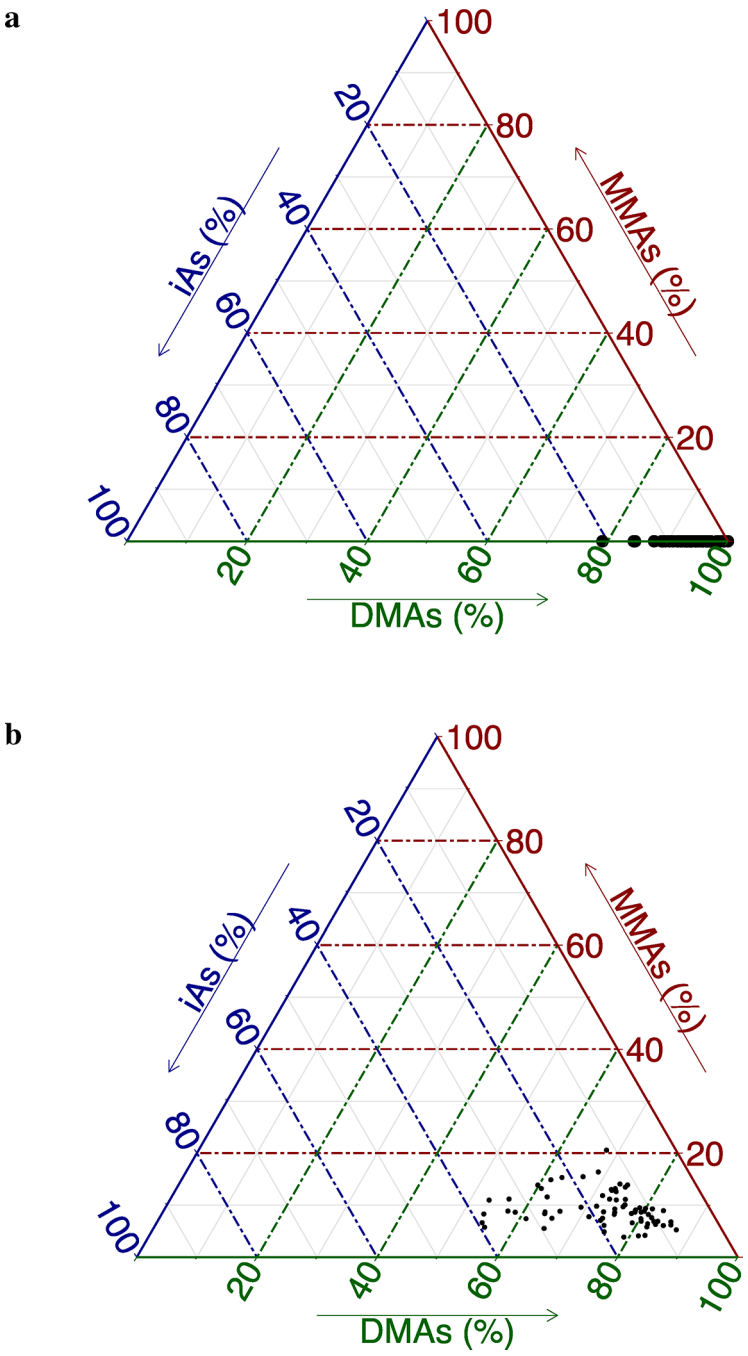

Fig. 7.

Ternary diagrams of As species visualizing the relative proportions of each As species in urine **a** and liver **b**. Each point on the simplex represents the distribution for a single sample. Each vertex represents one of the three As species and proximity to a vertex corresponds to a higher contribution of that species; **a** In urine, all samples had MMAs measure below the LOD and the composition is dominated by DMAs; **b** In liver, DMAs vs. iAs remains

the main axis of variation with DMAs dominating the composition. MMAs contributes very little to the composition

Table 1

Model selection results

Covariate	Metabolic indicator						
Baseline value	**FPI**	**PI15**	**FBG**	**BG15**	**HOMA-B**	**HOMA-IR**	**Ins. Index**
Week -1 indicator	□	■	■	■			
iAs exposure	□	□	□	□	□	□	□
Weight	■	■	□	□	■	■	
Fat	■	□		□			
iAs exposure x Fat	■	□					
iAs exposure x Weight					■	□	
Weight x Fat				■			
p-value(s)[a]	0.072, 0.003	0.547,0.099	0.309	0.157	0.548, 0.002	0.249, 0.084	0.077

Independent variables that remain after model selection are indicated with square symbols. A bold '■' indicates significance at the α=0.05 level, while an unfilled '□' indicates an insignificant retained variable; iAs was always retained regardless of significance

[a]Corresponds to a test of significance of the term(s) involving iAs; the p value associated with the main effect is always listed first, followed by the p value associated with the interaction term (when applicable)

Table 2

Relationships between iAs exposure and metabolic indicators

Indicator	iAs exposure		iAs exposure x %fat		iAs exposure x Weight		Covariates[a]
	Beta [95% CI]	p	Beta [95% CI]	p	Beta [95% CI]	p	
FPI	−0.16 [−0.32,0.01]	0.072	0.29 [0.11,0.47]	0.003			B, W, iAS, P, iAs*P
PI15	−0.05 [−0.21,0.11]		0.18 [−0.03,0.38]	0.099			B, W, iAs, P, iAs*P
FBG	−3.50 [−10.21,3.20]						B, W, iAs
BG15	−18.22 [−43.17,6.73]						B, W, iAs, P, W*P
HOMA-B	−91.72 [−389.80,206.36]				362.78 [139.32,586.24]	0.002	W, iAs, W*iAs
HOMA-IR	−5.94 [−15.96,4.08]				6.73 [−0.78,14.24]	0.084	W, iAs, W*iAs
Ins. Index	0.16 [−0.16,0.34]						iAs

A*B indicates an interaction between A and B

W body weight, *iAs* cumulative inorganic arsenic exposure, *P* percent body fat

[a] B = Baseline (week -1) indicator value